Variability of the M_2 internal tide in the South China Sea under climate change

Zheng Guo (Zhejiang Ocean University)
Xinyu Guo (CMES, Ehime University)

1. Purposes

Internal tides (ITs) play an important role in dissipating surface tidal energy and enhancing mixing. The magnitude and geography of IT mixing influence the global climate, including the global oceanic overturning circulation, water property distribution, and air-sea interactions. Moreover, as a ubiquitous motion in the global ocean, ITs also have major effects on acoustic transmission and oil-drilling platforms. In light of ITs' significant oceanographic effect, it's important to understand their changes. ITs in the South China Sea (SCS) show a temporal variation on different scales, where stratification plays an important role. The global stratification has strengthened by 5.3% during 1960−2018 and is expected to continue its increase trend in this century. The primary goal of this study is to explore how ITs will be affected by global warming.

2. Methods

2.1 Data for stratification analysis

In this study, we use simulation data under two shared socioeconomic pathways (SSPs) scenarios, i.e., SSP1-2.6 and SSP5-8.5, from CanESM5, one of the models that participate in the sixth phase of Coupled Model Intercomparison Project (CMIP6).

2.2 Settings of the Coastal and Regional Ocean COmmunity (CROCO) model

The CROCO model is used to explore the changes in ITs generation under different scenarios. The simulation domain covers the northern SCS and part of the Philippine Sea from 115.5−126.5°E and 16−26°N (Figure 1a). At the four open boundaries, the surface elevations and barotropic currents of the M_2 tide are introduced to force the model.

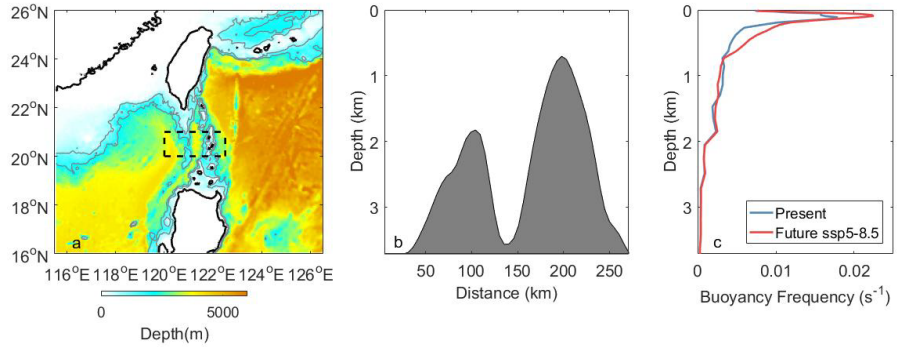

Figure 1. (a) Bathymetry of the CROCO simulation domain (shading, unit: m). (b) The meridionally averaged bathymetry of the middle LS used in the CELT simulation. (c) The mean buoyancy frequency within the middle LS used for the CELT Present and Future SSP5-8.5 experiments.

We conduct three experiments, i.e., the Present case, Future SSP1-2.6 case, and Future SSP5-8.5 case. Their initial fields are provided by the annual temperature, salinity, and currents from the SSP1-2.6 simulation of 2015, the SSP1-2.6 simulation of 2101, and the

SSP5-8.5 simulation of 2101, respectively.

2.3 Settings of the Coupling Equations for Linear Tides (CELT) model

The CELT model is used to investigate the mechanism behind changes in ITs generation within the LS against global warming. We use the meridionally averaged bathymetry of the middle LS (120°E-122.5°E, 20°N-21°N) in the CELT simulation (Figure 1b). Two groups of experiments are conducted: the Present cases and the Future SSP5-8.5 cases. Their stratifications are prescribed with data extracted from the SSP1-2.6 simulation of 2015 and SSP5-8.5 simulation of 2101, respectively (Figure 1c). In each group of experiments, simulation is conducted over three bathymetries, i.e., double ridges, single east ridge, and single west ridge.

3. Results

3.1 Changes in stratification

Attention is paid to the changes in the stratification, which plays an important role in the generation of ITs. Compared with the annual stratification profile in 2015 derived from the SSP1-2.6 simulation, the stratification anomaly in the upper 800 m under the SSP1-2.6 scenario shows a three-layer structure: the layer between 100 m and 200 m of negative anomaly is sandwiched between two layers of positive anomaly (Figure 2a). Under the SSP5-8.5 scenario, the stratification anomaly also shows a three-layer pattern (Figure 2b). However, the middle layer of negative anomaly becomes thinner towards the end of the 21st century and finally vanishes because the stratification intensifies across the whole water column. Averaged vertically, the variation of buoyancy frequency under the two scenarios are comparable in the first two decades. However, after 2040, the mean stratification remains relatively stable under the SSP1-2.6 scenario but shows a linear increase at a rate of 2.13×10^{-3} s^{-1} per century under the SSP5-8.5 scenario. The averaged stratification of the upper 800 m waters increases by 7.4% and 26.8% from 2015 to 2110 under the SSP1-2.6 and SSP5-8.5 scenarios, respectively.

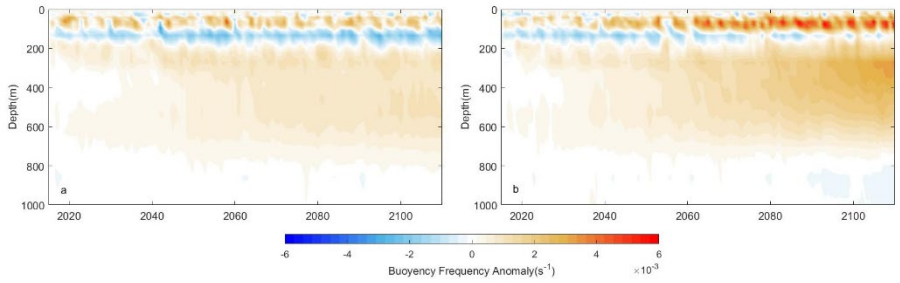

Figure 2. Time series of the stratification anomalies under the (a) SSP1-2.6 and (b) SSP5-8.5 scenarios relative to the 2015 stratification profile from the SSP1-2.6 simulation.

3.2 IT energy budgets

The two ridges in the LS are important generation sites of the M_2 ITs (Figure 3a). The generation of the M_2 ITs shows a decreasing trend with global warming (Figures 3b and 3c). Under the SSP1-2.6 scenario, the total generation of the M_2 ITs decreases by 2.7% from 17.49 GW to 17.02 GW in a century. Further inspection of the distribution of conversion rates shows that the amount of ITs generated decreases in most areas of the

middle LS. However, an increase in conversion rates is also noticed, especially in the northern part of the west ridge. Changes in conversion rates are more significant under the SSP5-8.5 scenario where the stratification shows a more remarkable change than that under the SSP 1-2.6 scenario. Although the generation of ITs strengthens in some areas, sharp decreases are seen in the middle LS. The ITs generated over the LS is 13.52 GW, amounting to a 22.7% decrease from the Present case.

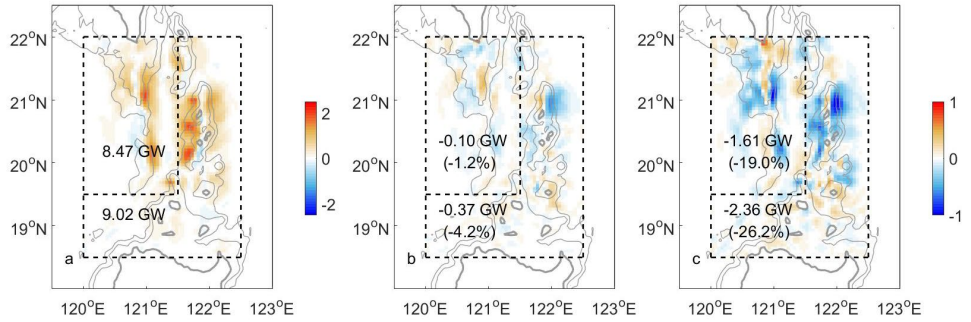

Figure 3. (a) Energy conversion rates of the M_2 ITs (shading, unit: W/m^2) in the present and its difference with those in the future (Future case minus Present case) under the (b) SSP1-2.6 and (c) SSP5-8.5 scenarios.

A large fraction of energy radiates away from the LS. Figure 4a shows that the pattern of depth-integrated energy flux of the M_2 ITs is consistent with previous studies. However, a reduction in barotropic to baroclinic energy conversion rates results in a reduction in energy flux received by the SCS and the Philippine Sea (Figures 4b and 4c). Under the SSP1-2.6 scenario, the westward ITs energy flux decreases by 7.1% to 4.05 GW, while the eastward fluxes change very slightly. Under the SSP5-8.5 scenario, all the three main ITs beams weaken significantly, resulting in sharp decreases of 30.9% and 25.3% in the ITs moving westwards and eastwards out of the LS, respectively.

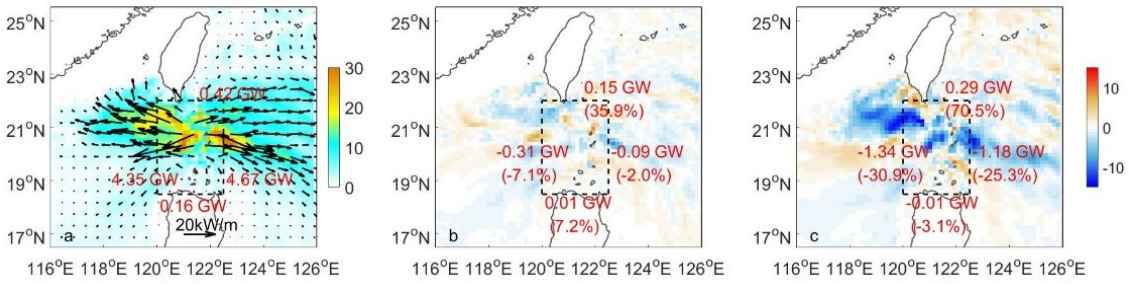

Figure 4. (a) Depth-integrated energy flux of the M_2 ITs in the Present case and its difference with those in the Future (Future case minus Present case) under the (b) SSP1-2.6 and (c) SSP5-8.5 scenarios.

3.3 Mechanism of ITs weakening

Results presented above show that the IT generation in the LS will be weakened as the ocean warms (stratification increases). It seems contradictory to the projection by the equation of 'Baines force', which indicates that the conversion of barotropic to baroclinic tides is directly proportional to N^2. To explore what happens within the LS in our simulation, we first extract the mean flow from the Present case and the Future cases under two scenarios. As is displayed in Figure 5, they have a similar pattern showing a

strong northward Kuroshio passing the LS in a leaping path. The similarity in the mean flow indicates that the difference in barotropic to baroclinic energy conversion rates largely results from the stratification. Stratification variation could change the interference of ITs in the LS by influencing the wavelength of ITs and finally change the barotropic-to-baroclinic energy conversion. Thereafter, we conduct another group of experiments based on the CELT model to validate the above speculation.

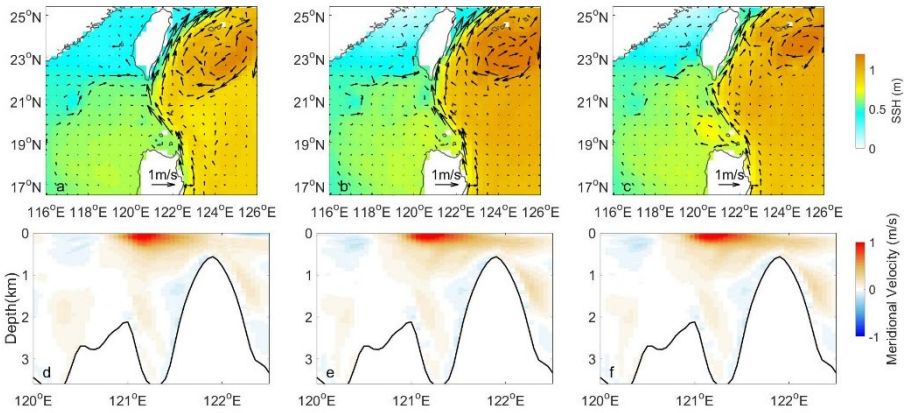

Figure 5. The (a-c) sea surface height (SSH, shading, unit: m) and mean flow (arrows, unit: m/s) in the simulation domain and (d-f) the meridional velocity (shading, unit: m/s) along the 20.5°N transection in the LS extracted from the (a, d) Present case, (b, e) Future SSP1-2.6 case, and (c, f) Future SSP5-8.5 case.

The CELT simulated amplitude of the horizontal velocity and energy flux of the M_2 ITs is shown in Figure 6. In the Present case, we could see the westwards-propagating ITs beam originates from the east flank of the east ridge and the weaker eastwards-propagating ITs beam originates from the top of the west ridge overlap after once reflection off the sea surface. The results from the Future SSP5-8.5 case over the double ridges show weaker energy flux than the Present case. In addition, the IT beam from the east flank of the east ridge reaches further to bounce at the west flank of the west ridge instead of its top, indicating that the wavelength of the M_2 ITs increases with the strengthening stratification. The path of the ITs from the west ridge also changes, not overlapping with that from the east ridge.

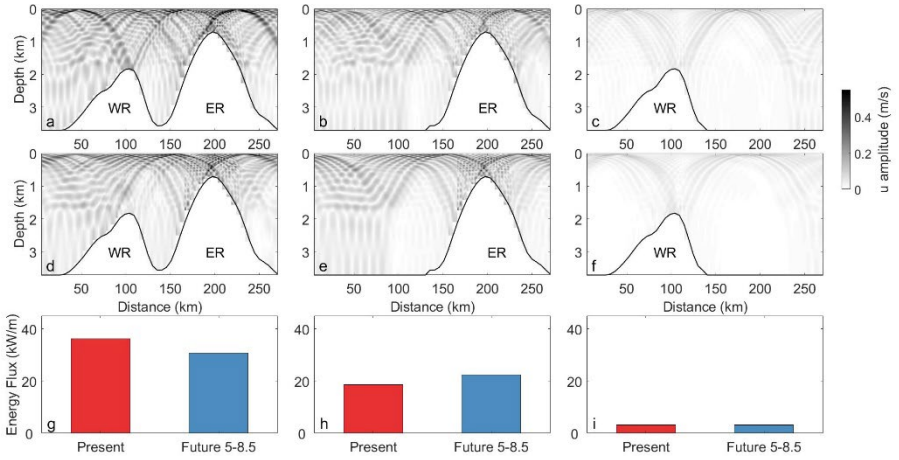

Figure 6. Amplitude of the horizontal velocity of the M_2 ITs in the CELT (a-c) Present

and (d-f) Future 5-8.5 cases simulated with the bathymetries of (a, d) double ridges, (b, e) single east ridge (ER), and (c, g) single west ridge (WR). (g-i) Magnitude of depth-integrated energy flux at the boundaries of the LS corresponding to the three topographies.

The energy flux of the M_2 ITs is integrated vertically to further quantify the difference between the two groups of experiments. The sum of values at both ends of the transection could be regarded as the amount of ITs generated within the LS, because dissipation is not considered in the CELT simulation. The variation in ITs generation over the bathymetry of double ridges is consistent with the CROCO simulation: the generation of ITs decreases as the stratification strengthens. Specifically, the ITs propagating out of LS is 30.84 kW/m in the Future 5-8.5 case, which decreases by 15% from the Present case. However, in the single-east-ridge experiment, stronger stratification results in stronger IT generation, which is consistent with the projection of theory. The generation of ITs is much weaker on the west ridge and shows little change. The reason might be that the west ridge is relatively low and stratification in the deep ocean remains nearly unchanged.

The opposite changes of ITs between the double-ridge and single-ridge experiments suggest the role of bathymetry. We measure the effect of interference in the CELT simulation by calculating the amplification ψ following:

$$\psi = \frac{F_{\mathrm{DR}} - (F_{\mathrm{WR}} + F_{\mathrm{ER}})}{F_{\mathrm{WR}} + F_{\mathrm{ER}}}, \tag{2}$$

where subscripts WR, ER, and DR refer to the west-ridge, east-ridge, and double-ridge cases. The amplifications in the Present case and Future 5-8.5 case are 0.66 and 0.21, respectively, which validates that the generation of the M_2 ITs decreases because their constructive interference within the LS weakens as the stratification strengthens.

3. Future challenges

Changes in the IT generation and propagation against climate change have significant implications. The ITs radiated from the LS are the dominant energy source for the tidal dissipation in the SCS. A sharp decrease in ITs will weaken diapycnal mixing in the domain, which will consequently influence the circulation in SCS and abyssal water transport through the LS. Near coasts where ITs break, nutrients delivered by ITs-induced mixing and subsequently growth of phytoplankton will decrease as ITs weaken. Further investigation is needed to estimate these effects.

Moreover, the changes of ITs in the LS is different from those in the Andaman Sea where increase in stratification will enhance ITs generation. It indicates that caution should be taken when predicting the changes of IT generation on a global scale under climate change. The site-dependent changes of ITs will yield a complex global geography of IT mixing. This pattern deserves more attention in the development of mixing parameterizations, because it affects the meridional overturning circulation and thus the broader global climate system.